Learning Neural Networks with Adaptive Regularization

Han Zhao*†, **Yao-Hung Hubert Tsai***†, **Ruslan Salakhutdinov**†, **Geoffrey J. Gordon**†‡
†Carnegie Mellon University, ‡Microsoft Research Montreal
{han.zhao,yaohungt,rsalakhu}@cs.cmu.edu
geoff.gordon@microsoft.com

Abstract

Feed-forward neural networks can be understood as a combination of an intermediate representation and a linear hypothesis. While most previous works aim to diversify the representations, we explore the complementary direction by performing an adaptive and data-dependent regularization motivated by the empirical Bayes method. Specifically, we propose to construct a matrix-variate normal prior (on weights) whose covariance matrix has a Kronecker product structure. This structure is designed to capture the correlations in neurons through backpropagation. Under the assumption of this Kronecker factorization, the prior encourages neurons to borrow statistical strength from one another. Hence, it leads to an adaptive and data-dependent regularization when training networks on small datasets. To optimize the model, we present an efficient block coordinate descent algorithm with analytical solutions. Empirically, we demonstrate that the proposed method helps networks converge to local optima with smaller stable ranks and spectral norms. These properties suggest better generalizations and we present empirical results to support this expectation. We also verify the effectiveness of the approach on multiclass classification and multitask regression problems with various network structures. Our code is publicly available at: `https://github.com/yaohungt/Adaptive-Regularization-Neural-Network`.

1 Introduction

Although deep neural networks have been widely applied in various domains [19, 25, 27], usually its parameters are learned via the principle of maximum likelihood, hence its success crucially hinges on the availability of large scale datasets. When training rich models on small datasets, explicit regularization techniques are crucial to alleviate overfitting. Previous works have explored various regularization [39] and data augmentation [19, 38] techniques to learn diversified representations. In this paper, we look into an alternative direction by proposing an adaptive and data-dependent regularization method to encourage neurons of the same layer to share statistical strength through exploiting correlations between data and gradients. The goal of our method is to prevent overfitting when training (large) networks on small dataset. Our key insight stems from the famous argument by Efron [8] in the literature of the empirical Bayes method: *It is beneficial to learn from the experience of others*. The empirical Bayes methods provide us a guiding principle to learn model parameters even if we do not have complete information about prior distribution. From an algorithmic perspective, we argue that the connection weights of neurons in the same layer (row/column vectors of the weight matrix) will be correlated with each other through the backpropagation learning. Hence, by learning the correlations of the weight matrix, a neuron can "borrow statistical strength" from other neurons in the same layer, which essentially increases the effective sample size during learning.

[*] Equal contribution.

As an illustrating example, consider a simple setting where the input $\mathbf{x} \in \mathbb{R}^d$ is fully connected to a hidden layer $\mathbf{h} \in \mathbb{R}^p$, which is further fully connected to the single output $\hat{y} \in \mathbb{R}$. Let $\sigma(\cdot)$ be the nonlinear activation function, e.g., ReLU [33], $W \in \mathbb{R}^{p\times d}$ be the connection matrix between the input layer and the hidden layer, and $\mathbf{a} \in \mathbb{R}^p$ be the vector connecting the output and the hidden layer. Without loss of generality, ignoring the bias term in each layer, we have: $\hat{y} = \mathbf{a}^T\mathbf{h}, \mathbf{h} = \sigma(W\mathbf{x})$. Consider using the usual ℓ_2 loss function $\ell(\hat{y}, y) = \frac{1}{2}|\hat{y} - y|^2$ and take the derivative of $\ell(\hat{y}, y)$ w.r.t. W. We obtain the update formula in backpropagation as $W \leftarrow W - \alpha(\hat{y} - y)(\mathbf{a} \circ \mathbf{h}')\,\mathbf{x}^T$, where $\mathbf{h}'$ is the component-wise derivative of $\mathbf{h}$ w.r.t. its input argument, and $\alpha > 0$ is the learning rate. Realize that $(\mathbf{a} \circ \mathbf{h}')\,\mathbf{x}^T$ is a rank 1 matrix, and the component of $\mathbf{h}'$ is either 0 or 1. Hence, the update for each row vector of W is linearly proportional to $\mathbf{x}$. Similar observation also holds for each column vector of W, so it implies that the row/column vectors of W are correlated with each other through learning. Although in this example we only discuss a one-hidden-layer network, it is straightforward to verify that the gradient update formula for general feed-forward networks admits the same rank one structure. The above observation leads us to the following question:

Can we define a prior distribution over W that captures the correlations through the learning process for better generalization?

Our Contributions To answer the above question, we develop an adaptive regularization method for neural nets inspired by the empirical Bayes method. Motivated by the example above, we propose a matrix-variate normal prior whose covariance matrix admits a Kronecker product structure to capture the correlations between different neurons. Using tools from convex analysis, we present an efficient block coordinate descent algorithm with closed-form solutions to optimize the model. Empirically, we show the proposed method helps the network converge to local optima with smaller stable ranks and spectral norms, and we verify the effectiveness of the approach on both multiclass classification and multitask regression problems with various network structures.

2 Preliminary

Notation and Setup We use lowercase letter to represent scalar and lowercase bold letter to denote vector. Capital letter, e.g., X, is reserved for matrix. Calligraphic letter, such as $\mathcal{D}$, is used to denote set. We write $\mathrm{Tr}(A)$ as the trace of a matrix A, $\det(A)$ as the determinant of A and $\mathrm{vec}(A)$ as A's vectorization by column. $[n]$ is used to represent the set $\{1, \dots, n\}$ for any integer n. Other notations will be introduced whenever needed. Suppose we have access to a training set $\mathcal{D}$ of n pairs of data instances $(\mathbf{x}_i, y_i), i \in [n]$. We consider the supervised learning setting where $\mathbf{x}_i \in \mathcal{X} \subseteq \mathbb{R}^d$ and $y_i \in \mathcal{Y}$. Let $p(y \mid \mathbf{x}, \mathbf{w})$ be the conditional distribution of y given $\mathbf{x}$ with parameter $\mathbf{w}$. The parametric form of the conditional distribution is assumed be known. In this paper, we assume the model parameter $\mathbf{w}$ is sampled from a prior distribution $p(\mathbf{w} \mid \theta)$ with hyperparameter θ. On the other hand, given $\mathcal{D}$, the posterior distribution of $\mathbf{w}$ is denoted by $p(\mathbf{w} \mid \mathcal{D}, \theta)$.

The Empirical Bayes Method To compute the predictive distribution, we need access to the value of the hyperparameter θ. However, complete information about the hyperparameter θ is usually not available in practice. To this end, empirical Bayes method [1, 9, 10, 12, 36] proposes to estimate θ from the data directly using the marginal distribution:

$$\hat{\theta} = \arg\max_{\theta}\ p(\mathcal{D} \mid \theta) = \arg\max_{\theta} \int p(\mathcal{D} \mid \mathbf{w}) \cdot p(\mathbf{w} \mid \theta)\; d\mathbf{w}. \tag{1}$$

Under specific choice of the likelihood function $p(\mathbf{x}, y \mid \mathbf{w})$ and the prior distribution $p(\mathbf{w} \mid \theta)$, e.g., conjugate pairs, we can solve the above integral in closed form. In certain cases we can even obtain an analytic solution of $\hat{\theta}$, which can then be plugged into the prior distribution. At a high level, by learning the hyperparameter θ in the prior distribution directly from data, the empirical Bayes method provides us a principled and data-dependent way to obtain an estimator of $\mathbf{w}$. In fact, when both the prior and the likelihood functions are normal, it has been formally shown that the empirical Bayes estimators, e.g., the James-Stein estimator [23] and the Efron-Morris estimator [11], dominate the classic maximum likelihood estimator (MLE) in terms of quadratic loss for every choice of the model parameter $\mathbf{w}$. At a colloquial level, the success of the empirical Bayes method can be attributed to the effect of *"borrowing statistical strength"* [8], which also makes it a powerful tool in multitask learning [28, 43] and meta-learning [15].

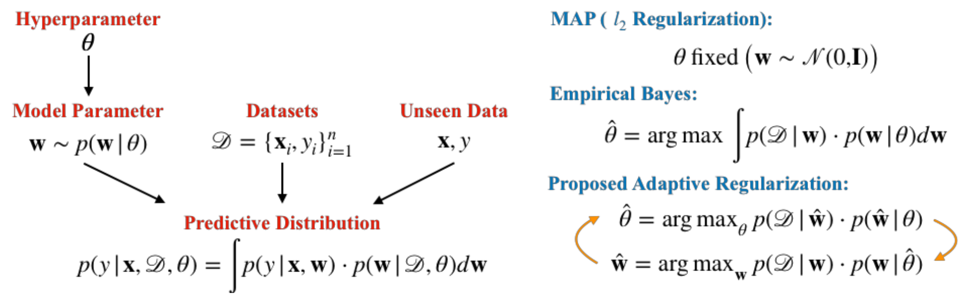
Hyperparameter
θ
Model Parameter
$\mathbf{w} \sim p(\mathbf{w} \mid \theta)$
Datasets
$\mathscr{D} = \{\mathbf{x}_i, y_i\}_{i=1}^n$
Unseen Data
$\mathbf{x}, y$
Predictive Distribution
$p(y \mid \mathbf{x}, \mathscr{D}, \theta) = \int p(y \mid \mathbf{x}, \mathbf{w}) \cdot p(\mathbf{w} \mid \mathscr{D}, \theta) d\mathbf{w}$
MAP (l_2 Regularization):
θ fixed $(\mathbf{w} \sim \mathscr{N}(0, \mathbf{I}))$
Empirical Bayes:
$\hat{\theta} = \arg\max \int p(\mathscr{D} \mid \mathbf{w}) \cdot p(\mathbf{w} \mid \theta) d\mathbf{w}$
Proposed Adaptive Regularization:
$\hat{\theta} = \arg\max_\theta p(\mathscr{D} \mid \hat{\mathbf{w}}) \cdot p(\hat{\mathbf{w}} \mid \theta)$
$\hat{\mathbf{w}} = \arg\max_\mathbf{w} p(\mathscr{D} \mid \mathbf{w}) \cdot p(\mathbf{w} \mid \hat{\theta})$
Figure 1: Illustration for Bayes/ Empirical Bayes, and our proposed adaptive regularization.

3 Learning with Adaptive Regularization

In this section we first propose an adaptive regularization (AdaReg) method, which is inspired by the empirical Bayes method, for learning neural networks. We then combine our observation in Sec. 1 to develop an efficient adaptive learning algorithm with matrix-variate normal prior. Through our derivation, we provide several connections and interpretations with other learning paradigms.

3.1 The Proposed Adaptive Regularization

When the likelihood function $p(\mathcal{D} \mid \mathbf{w})$ is implemented as a neural network, the marginalization in (1) over model parameter $\mathbf{w}$ cannot be computed exactly. Nevertheless, instead of performing expensive Monte-Carlo simulation, we propose to estimate both the model parameter $\mathbf{w}$ and the hyperparameter θ in the prior simultaneously from the joint distribution $p(\mathcal{D}, \mathbf{w} \mid \theta) = p(\mathcal{D} \mid \mathbf{w}) \cdot p(\mathbf{w} \mid \theta)$. Specifically, given an estimate $\hat{\mathbf{w}}$ of the model parameter, by maximizing the joint distribution w.r.t. θ, we can obtain $\hat{\theta}$ as an approximation of the maximum marginal likelihood estimator. As a result, we can use $\hat{\theta}$ to further refine the estimate $\hat{\mathbf{w}}$ by maximizing the posterior distribution as follows:

$$\hat{\mathbf{w}} \leftarrow \max_{\mathbf{w}} \; p(\mathbf{w} \mid \mathcal{D}) = \max_{\mathbf{w}} \; p(\mathcal{D} \mid \mathbf{w}) \cdot p(\mathbf{w} \mid \hat{\theta}). \tag{2}$$

The maximizer of (2) can in turn be used in an updated joint distribution. Formally, we can define the following optimization problem that characterizes our Adaptive Regularization (AdaReg) framework:

$$\max_{\mathbf{w}} \max_{\theta} \; \log p(\mathcal{D} \mid \mathbf{w}) + \log p(\mathbf{w} \mid \theta). \tag{3}$$

It is worth connecting the optimization problem (3) to the classic maximum a posteriori (MAP) inference and also discuss their difference. If we drop the inner optimization over the hyperparameter θ in the prior distribution. Then for any fixed value $\hat{\theta}$, (3) reduces to MAP with the prior defined by the specific choice of $\hat{\theta}$, and the maximizer $\hat{\mathbf{w}}$ corresponds to the mode of the posterior distribution given by $\hat{\theta}$. From this perspective, the optimization problem in (3) actually defines a series of MAP inference problems, and the sequence $\{\hat{\mathbf{w}}_j(\hat{\theta}_j)\}_j$ defines a solution path towards the final model parameter. On the algorithmic side, the optimization problem (3) also suggests a natural block coordinate descent algorithm where we alternatively optimize over $\mathbf{w}$ and θ until the convergence of the objective function. An illustration of the framework is shown in Fig. 1.

3.2 Neural Network with Matrix-Normal Prior

Inspired by the observation from Sec. 1, we propose to define a matrix-variate normal distribution [16] over the connection weight matrix W: $W \sim \mathcal{MN}(0_{p\times d}, \Sigma_r, \Sigma_c)$, where $\Sigma_r \in \mathbb{S}_{++}^p$ and $\Sigma_c \in \mathbb{S}_{++}^d$ are the row and column covariance matrices, respectively.[2] Equivalently, one can understand the matrix-variate normal distribution over W as a multivariate normal distribution with a Kronecker product covariance structure over $\mathrm{vec}(W)$: $\mathrm{vec}(W) \sim \mathcal{N}(0_{p\times d}, \Sigma_c \otimes \Sigma_r)$. It is then easy to check that the marginal prior distributions over the row and column vectors of W are given by:

$$W_{i:} \sim \mathcal{N}(\mathbf{0}_d, [\Sigma_r]_{ii} \cdot \Sigma_c), \quad W_{:j} \sim \mathcal{N}(\mathbf{0}_p, [\Sigma_c]_{jj} \cdot \Sigma_r).$$

[2]The probability density function is given by $p(W \mid \Sigma_r, \Sigma_c) = \frac{\exp\left(-\operatorname{Tr}(\Sigma_r^{-1} W \Sigma_c^{-1} W^T)/2\right)}{(2\pi)^{pd/2} \det(\Sigma_r)^{d/2} \det(\Sigma_c)^{p/2}}$.

We point out that the Kronecker product structure of the covariance matrix exactly captures our prior about the connection matrix W: the fan-in/fan-out of neurons in the same layer (row/column vectors of W) are correlated with the same correlation matrix in the prior, and they only differ at the scales.

For illustration purpose, let us consider the simple feed-forward network discussed in Sec. 1. Consider a reparametrization of the model by defining $\Omega_r := \Sigma_r^{-1}$ and $\Omega_c := \Sigma_c^{-1}$ to be the corresponding precision matrices and plug in the prior distribution into the our AdaReg framework (see (3)). After routine algebraic simplifications, we reach the following concrete optimization problem:

$$\begin{aligned}\min_{W,\mathbf{a}}\min_{\Omega_r,\Omega_c} \quad & \frac{1}{2n}\sum_{i\in[n]}(\hat{y}(\mathbf{x}_i;W,\mathbf{a})-y_i)^2+\lambda||\Omega_r^{1/2}W\Omega_c^{1/2}||_F^2-\lambda\big(d\log\det(\Omega_r)+p\log\det(\Omega_c)\big)\\ \text{subject to} \quad & uI_p\preceq\Omega_r\preceq vI_p,\ uI_d\preceq\Omega_c\preceq vI_d\end{aligned} \tag{4}$$

where λ is a constant that only depends on p and d, $0<u\leq v$ and $uv=1$. Note that the constraint is necessary to guarantee the feasible set to be compact so that the optimization problem is well formulated and a minimum is attainable. [3] It is not hard to show that in general the optimization problem (4) is not jointly convex in terms of $\{\mathbf{a},W,\Omega_r,\Omega_c\}$, and this holds even if the activation function is linear. However, as we will show later, for any fixed $\mathbf{a},W$, the reparametrization makes the partial optimization over Ω_r and Ω_c bi-convex. More importantly, we can derive an efficient algorithm that finds the optimal $\Omega_r(\Omega_c)$ for any fixed $\mathbf{a},W,\Omega_c(\Omega_r)$ in $O(\max\{d^3,p^3\})$ time with closed form solutions. This allows us to apply our algorithm to networks of large sizes, where a typical hidden layer can contain thousands of nodes. Note that this is in contrast to solving a general semi-definite programming (SDP) problem using black-box algorithm, e.g., the interior-point method [32], which is computationally intensive and hard to scale to networks with moderate sizes. Before we delve into the details on solving (4), it is instructive to discuss some of its connections and differences to other learning paradigms.

Maximum-A-Posteriori Estimation. Essentially, for model parameter W, (4) defines a sequence of MAP problems where each MAP is indexed by the pair of precision matrices $(\Omega_r^{(t)},\Omega_c^{(t)})$ at iteration t. Equivalently, at each stage of the optimization, we can interpret (4) as placing a matrix variate normal prior on W where the precision matrix in the prior is given by $\Omega_r^{(t)}\otimes\Omega_c^{(t)}$. From this perspective, if we fix $\Omega_r^{(t)}=I_p$ and $\Omega_c^{(t)}=I_d$, $\forall t$, then (4) naturally reduces to learning with ℓ_2 regularization [26]. More generally, for non-diagonal precision matrices, the regularization term for W becomes:

$$||\Omega_r^{1/2}W\Omega_c^{1/2}||_F^2=||\text{vec}(\Omega_r^{1/2}W\Omega_c^{1/2})||_2^2=||(\Omega_c^{1/2}\otimes\Omega_r^{1/2})\ \text{vec}(W)||_2^2,$$

and this is exactly the Tikhonov regularization [13] imposed on W where the Tikhonov matrix Γ is given by $\Gamma:=\Omega_c^{1/2}\otimes\Omega_r^{1/2}$. But instead of manually designing the regularization matrix Γ to improve the conditioning of the estimation problem, we propose to also learn both precision matrices (so Γ as well) from data. From an algorithmic perspective, $\Gamma^T\Gamma=\Omega_c\otimes\Omega_r$ serves as a preconditioning matrix w.r.t. model parameter W to reshape the gradient according to the geometry of the data [7, 17, 18].

Volume Minimization. Let us consider the $\log\det(\cdot)$ function over the positive definite cone. It is well known that the log-determinant function is concave [3]. Hence for any pair of matrices $A_1,A_2\in\mathbb{S}_{++}^m$, the following inequality holds:

$$\log\det(A_1)\leq\log\det(A_2)+\langle\nabla\log\det(A_2),A_1-A_2\rangle=\log\det(A_2)+\text{Tr}(A_2^{-1}A_1)-m. \tag{5}$$

Applying the above inequality twice by fixing $A_1=W\Omega_cW^T/2d, A_2=\Sigma_r$ and $A_1=W^T\Omega_rW/2p, A_2=\Sigma_c$ respectively leads to the following inequalities:

$$\begin{aligned}d\log\det(W\Omega_cW^T/2d)&\leq-d\log\det(\Omega_r)+\frac{1}{2}\text{Tr}(\Omega_rW\Omega_cW^T)-dp,\\ p\log\det(W^T\Omega_rW/2p)&\leq-p\log\det(\Omega_c)+\frac{1}{2}\text{Tr}(\Omega_rW\Omega_cW^T)-dp.\end{aligned}$$

Realize $\text{Tr}(\Omega_rW\Omega_cW^T)=||\Omega_r^{1/2}W\Omega_c^{1/2}||_F^2$. Summing the above two inequalities leads to:

$$d\log\det(W\Omega_cW^T)+p\log\det(W^T\Omega_rW)\leq||\Omega_r^{1/2}W\Omega_c^{1/2}||_F^2-\big(d\log\det(\Omega_r)+p\log\det(\Omega_c)\big)+c, \tag{6}$$

where c is a constant that only depends on d and p. Recall that $|\det(A^TA)|$ computes the squared volume of the parallelepiped spanned by the column vectors of A. Hence (6) gives us a natural

[3]The constraint $uv=1$ is only for the ease of presentation in the following part and can be readily removed.

interpretation of the objective function in (4): the regularizer essentially upper bounds the log-volume of the two parallelpipeds spanned by the row and column vectors of W. But instead of measuring the volume using standard Euclidean inner product, it also takes into account the local curvatures defined by Σ_r and Σ_c, respectively. For vectors with fixed lengths, the volume of the parallelepiped spanned by them becomes smaller when they are more linearly correlated, either positively or negatively. At a colloquial level, this means that the regularizer in (4) forces fan-in/fan-out of neurons at the same layer to be either positively or negatively correlated with each other, and this corresponds exactly to the effect of sharing statistical strengths.

3.3 The Algorithm

In this section we describe a block coordinate descent algorithm to optimize the objective function in (4) and detail how to efficiently solve the matrix optimization subproblems in closed form using tools from convex analysis. Due to space limit, we defer proofs and detailed derivation to appendix. Given a pair of constants $0 < u \leq v$, we define the following thresholding function $\mathbb{T}_{[u,v]}(x)$:

$$\mathbb{T}_{[u,v]}(x) := \max\{u, \min\{v, x\}\}. \tag{7}$$

We summarize our block coordinate descent algorithm to solve (4) in Alg. 1. In each iteration, Alg. 1 takes a first-order algorithm $\mathfrak{A}$, e.g., the stochastic gradient descent, to optimize the parameters of the neural network by backpropagation. It then proceeds to compute the optimal solutions for Ω_r and Ω_c using INVTHRESHOLD as a sub-procedure. Alg. 1 terminates when a stationary point is found.

We now proceed to show that the procedure INVTHRESHOLD finds the optimal solution given all the other variables fixed. Due to the symmetry between Ω_r and Ω_c in (4), we will only prove this for Ω_r, and similar arguments can be applied to Ω_c as well. Fix both W, Ω_c and ignore all the terms that do not depend on Ω_r, the sub-problem on optimizing Ω_r becomes:

$$\min_{\Omega_r} \quad \mathrm{Tr}(\Omega_r W \Omega_c W^T) - d \log\det(\Omega_r), \qquad \text{subject to} \quad uI_p \preceq \Omega_r \preceq vI_p. \tag{8}$$

It is not hard to show that the optimization problem (9) is convex. Define the constraint set $\mathcal{C} := \{A \in \mathbb{S}^p_{++} \mid uI_p \preceq A \preceq vI_p\}$ and the indicator function $\mathbb{I}_{\mathcal{C}}(A) = 0$ iff $A \in \mathcal{C}$ else ∞. Given the convexity of (9), we can use the indicator function to first transform (9) into the following unconstrained one:

$$\min_{\Omega_r} \quad \mathrm{Tr}(\Omega_r W \Omega_c W^T) - d \log\det(\Omega_r) + \mathbb{I}_{\mathcal{C}}(\Omega_r). \tag{9}$$

Then we can use the first-order optimality condition to characterize the optimal solution:

$$0 \in \partial\left(\frac{1}{d}\mathrm{Tr}(\Omega_r W \Omega_c W^T) - \log\det(\Omega_r) + \mathbb{I}_{\mathcal{C}}(\Omega_r)\right) = W\Omega_c W^T/d - \Omega_r^{-1} + \mathcal{N}_{\mathcal{C}}(\Omega_r),$$

where $\mathcal{N}_{\mathcal{C}}(A) := \{B \in \mathbb{S}^p \mid \mathrm{Tr}(B^T(Z - A)) \leq 0, \forall Z \in \mathcal{C}\}$ is the normal cone w.r.t. $\mathcal{C}$ at A. The following key lemma characterizes the structure of the normal cone:

Lemma 1. Let $\Omega_r \in \mathcal{C}$, then $\mathcal{N}_{\mathcal{C}}(\Omega_r) = -\mathcal{N}_{\mathcal{C}}(\Omega_r^{-1})$.

Equivalently, combining Lemma 1 with the optimality condition, we have

$$W\Omega_c W^T/d - \Omega_r^{-1} \in \mathcal{N}_{\mathcal{C}}(\Omega_r^{-1}).$$

Geometrically, this means that the optimum Ω_r^{-1} is the Euclidean projection of $W\Omega_c W^T/d$ onto $\mathcal{C}$. Hence in order to solve (9), it suffices if we can solve the following Euclidean projection problem efficiently, where $\widetilde{\Omega_r} \in \mathbb{S}^p$ is a given real symmetric matrix:

$$\min_{\Omega_r} \quad ||\Omega_r - \widetilde{\Omega_r}||_F^2, \qquad \text{subject to} \quad uI_p \preceq \Omega_r \preceq vI_p. \tag{10}$$

Perhaps a little bit surprising, we can find the optimal solution to the above Euclidean projection problem efficiently in closed form:

Theorem 1. Let $\widetilde{\Omega_r} \in \mathbb{S}^p$ with eigendecomposition as $\widetilde{\Omega_r} = Q\Lambda Q^T$ and $\mathrm{Proj}_{\mathcal{C}}(\cdot)$ be the Euclidean projection operator onto $\mathcal{C}$, then $\mathrm{Proj}_{\mathcal{C}}(\widetilde{\Omega_r}) = Q\mathbb{T}_{[u,v]}(\Lambda)Q^T$.

Corollary 1. Let $W\Omega_c W^T$ be eigendecomposed as $Q\mathrm{diag}(\mathbf{r})Q^T$, then the optimal solution to (9) is given by $Q\mathbb{T}_{[u,v]}(d/\mathbf{r})Q^T$.

Similar arguments can be made to derive the solution for Ω_c in (4). The final algorithm is very simple as it only contains one SVD, hence its time complexity is $O(\max\{d^3, p^3\})$. Note that the total number of parameters in the network is at least $\Omega(dp)$, hence the algorithm is efficient as it scales sub-quadratically in terms of number of parameters in the network.

Algorithm 1 Block Coordinate Descent for Adaptive Regularization

```
Input: Initial value $\phi^{(0)} := \{\mathbf{a}^{(0)}, W^{(0)}\}$, $\Omega_r^{(0)} \in \mathbb{S}_{++}^p$ and $\Omega_c^{(0)} \in \mathbb{S}_{++}^d$, first-order optimization algorithm $\mathfrak{A}$.
 1: for $t = 1, \ldots, \infty$ until convergence do
 2:     Fix $\Omega_r^{(t-1)}$, $\Omega_c^{(t-1)}$, optimize $\phi^{(t)}$ by backpropagation and algorithm $\mathfrak{A}$
 3:     $\Omega_r^{(t)} \leftarrow \textsc{InvThreshold}(W^{(t)}\Omega_c^{(t-1)}W^{(t)T}, d, u, v)$
 4:     $\Omega_c^{(t)} \leftarrow \textsc{InvThreshold}(W^{(t)T}\Omega_r^{(t)}W^{(t)}, p, u, v)$
 5: end for
 6: procedure $\textsc{InvThreshold}(\Delta, m, u, v)$
 7:     Compute SVD: $Q\text{diag}(\mathbf{r})Q^T = \text{SVD}(\Delta)$
 8:     Hard thresholding $\mathbf{r}' \leftarrow \mathbb{T}_{[u,v]}(m/\mathbf{r})$
 9:     return $Q\text{diag}(\mathbf{r}')Q^T$
10: end procedure
```

4 Experiments

In this section we demonstrate the effectiveness of AdaReg in learning practical deep neural networks on real-world datasets. We report generalization, optimization as well as stability results.

4.1 Experimental Setup

Multiclass Classification (MNIST & CIFAR10): In this experiment, we show that AdaReg provides an effective regularization on the network parameters. To this end, we use a convolutional neural network as our baseline model. To show the effect of regularization, we gradually increase the training set size. In MNIST we use the step from 60 to 60,000 (11 different experiments) and in CIFAR10 we consider the step from 5,000 to 50,000 (10 different experiments). For each training set size, we repeat the experiments for 10 times. The mean along with its standard deviation are shown as the statistics. Moreover, since both the optimization and generalization of neural networks are sensitive to the size of minibatches [14, 24], we study two minibatch settings for 256 and 2048, respectively. In our method, we place a matrix-variate normal prior over the weight matrix of the last softmax layer, and we use Alg. 1 to optimize both the model weights and two covariance matrices.

Multitask Regression (SARCOS): SARCOS relates to an inverse dynamics problem for a seven degree-of-freedom (DOF) SARCOS anthropomorphic robot arm [41]. The goal of this task is to map from a 21-dimensional input space (7 joint positions, 7 joint velocities, 7 joint accelerations) to the corresponding 7 joint torques. Hence there are 7 tasks and the inputs are shared among all the tasks. The training set and test set contain 44,484 and 4,449 examples, respectively. Again, we apply AdaReg on the last layer weight matrix, where each row corresponds to a separate task vector.

We compare AdaReg with classic regularization methods in the literature, including weight decay, dropout [39], batch normalization (BN) [22] and the DeCov method [6]. We also note that we fix all the hyperparameters such as learning rate to be the same for all the methods. We report evaluation metrics on test set as a measure of generalization. To understand how the proposed adaptive regularization helps in optimization, we visualize the trajectory of the loss function during training. Lastly, we also present the inferred correlation of the weight matrix for qualitative study.

4.2 Results and Analysis

Multiclass Classification (MNIST & CIFAR10): Results on the multiclass classification for different training sizes are show in Fig. 2. For both MNIST and CIFAR10, we find AdaReg, Weight Decay, and Dropout are the effective regularization methods, while Batch Normalization and DeCov vary in different settings. Batch Normalization suffers from large batch size in CIFAR10 (comparing Fig. 2 (c) and (d)) but is not sensitive to batch size in MNIST (comparing Fig. 2 (a) and (b)). The performance deterioration in large batch size of Batch Normalization is also observed by [21]. DeCov, on the other hand, improves the generalization in MNIST with batch size 256 (see Fig. 2 (a)), while it demonstrates only comparable or even worse performance in other settings. To conclude, as training set size grows, AdaReg consistently performs better generalization as comparing to other regularization methods. We also note that AdaReg is not sensitive to the size of minibatches while most of the methods suffer from large minibatches. In appendix, we show the combination of AdaReg with other generalization methods can usually lead to even better results.

Table 1: Explained variance of different methods on 7 regression tasks from the SARCOS dataset.

Method	1st	2nd	3rd	4th	5th	6th	7th
MTL	0.4418	0.3472	0.5222	0.5036	0.6024	0.4727	0.5298
MTL-Dropout	0.4413	0.3271	0.5202	0.5063	0.6036	0.4711	0.5345
MTL-BN	0.4768	0.3770	0.5396	0.5216	0.6117	0.4936	0.5479
MTL-DeCoV	0.4027	0.3137	0.4703	0.4515	0.5229	0.4224	0.4716
MTL-AdaReg	**0.4769**	**0.3969**	**0.5485**	**0.5308**	**0.6202**	**0.5085**	**0.5561**

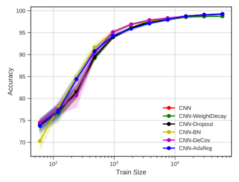

(a) MNIST (Batch Size: 256)

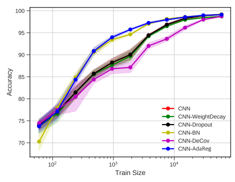

(b) MNIST (Batch Size: 2048)

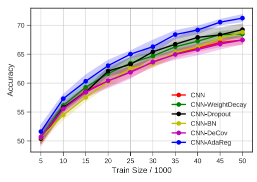

(c) CIFAR10 (Batch Size: 256)

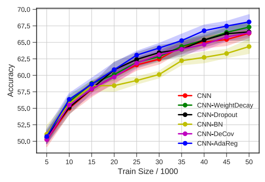

(d) CIFAR10 (Batch Size: 2048)

Figure 2: Generalization performance on MNIST and CIFAR10. AdaReg improves generalization under both minibatch settings.

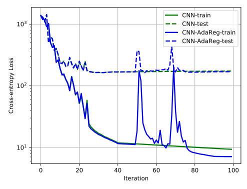

(a) T/B: 600/256

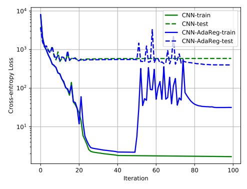

(b) T/B: 6000/256

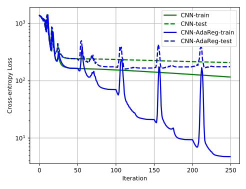

(c) T/B: 600/2048

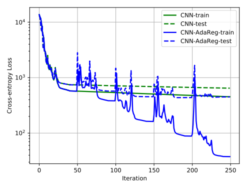

(d) T/B: 6000/2048

Figure 3: Optimization trajectory of AdaReg on MNIST with training size/batch size on training and test sets. AdaReg helps to converge to better local optima. Note the log-scale on y-axis.

Multitask Regression (SARCOS): In this experiment we are interested in investigating whether AdaReg can lead to better generalization for multiple related regression problems. To do so, we report the explained variance as a normalized metric, e.g., one minus the ratio between mean squared error and the variance of different methods in Table 1. The larger the explained variance, the better the predictive performance. In this case we observe a consistent improvement of AdaReg over other competitors on all the 7 regression tasks. We would like to emphasize that all the experiments share exactly the same experimental protocol, including network structure, optimization algorithm, training iteration, etc, so that the performance differences can only be explained by different ways of regularizations. For better visualization, we also plot the result in appendix.

Optimization: It has recently been empirically shown that BN helps optimization not by reducing internal covariate shift, but instead by smoothing the landscape of the loss function [37]. To understand how AdaReg improves generalization, in Fig. 3, we plot the values of the cross entropy loss function on both the training and test sets during optimization using Alg. 1. The experiment is performed in MNIST with batch size 256/2048. In this experiment, we fix the number of outer loop to be 2/5 and each block optimization over network weights contains 50 epochs. Because of the stochastic optimization over model weights, we can see several unstable peaks in function value around iteration 50 when trained with AdaReg, which corresponds to the transition phase between two consecutive outer loops with different row/column covariance matrices. In all the cases AdaReg converges to better local optima of the loss landscape, which lead to better generalization on the test set as well because they have smaller loss values on the test set when compared with training without AdaReg.

Stable rank and spectral norm: Given a matrix W, the stable rank of W, denoted as $\text{srank}(W)$, is defined as $\text{srank}(W) := ||W||_F^2/||W||_2^2$. As its name suggests, the stable rank is more stable than the rank because it is largely unaffected by tiny singular values. It has recently been shown [34, Theorem 1] that the generalization error of neural networks crucially depends on both the stable ranks and the spectral norms of connection matrices in the network. Specifically, it can be shown that the generalization error is upper bounded by $O\left(\sqrt{\prod_{j=1}^L ||W_j||_2^2 \sum_{j=1}^L \text{srank}(W_j)/n}\right)$, where L is the

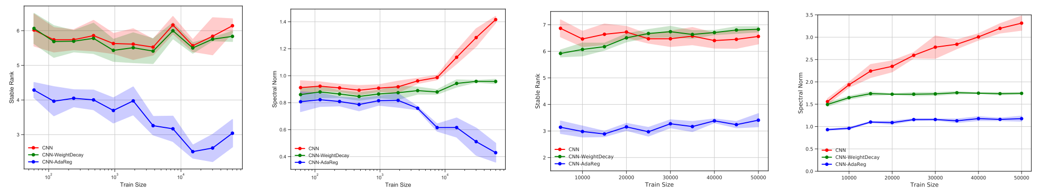

(a) MNIST: S. rank (b) MNIST: S. norm (c) CIFAR10: S. rank (d) CIFAR10: S. norm

Figure 4: Comparisons of stable ranks (S. rank) and spectral norms (S. norm) from different methods on MNIST and CIFAR10. x-axis corresponds to the training size.

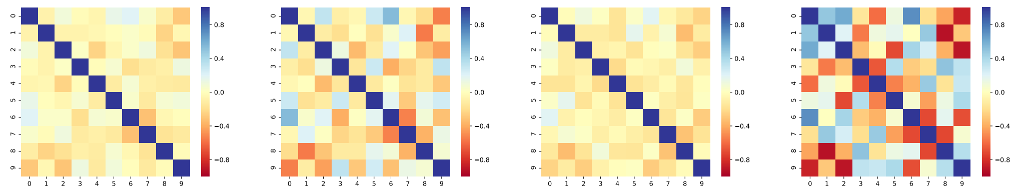

(a) CNN, Acc: 89.34 (b) AdaReg, Acc: 92.50 (c) CNN, Acc: 98.99 (d) AdaReg, Acc: 99.19

Figure 5: Correlation matrix of the weight matrix in the softmax layer. The left two correspond to dataset with training size 600 and the right two with size 60,000. Acc means the test set accuracy.

number of layers in the network. Essentially, this upper bound suggests that smaller spectral norm (smoother function mapping) and stable rank (skewed spectrum) leads to better generalization.

To understand why AdaReg improves generalization, in Fig. 4, we plot both the stable rank and the spectral norm of the weight matrix in the last layer of the CNNs used in our MNIST and CIFAR10 experiments. We compare 3 methods: CNN without any regularization, CNN trained with weight decay and CNN with AdaReg. For each setting we repeat the experiments for 5 times, and we plot the mean along with its standard deviation. From Fig. 4a and Fig. 4c it is clear that AdaReg leads to a significant reduction in terms of the stable rank when compared with weight decay, and this effect is consistent in all the experiments with different training size. Similarly, in Fig. 4b and Fig. 4d we plot the spectral norm of the weight matrix. Again, both weight decay and AdaReg help reduce the spectral norm in all settings, but AdaReg plays a more significant role than the usual weight decay. Combining the experiments with the generalization upper bound introduced above, we can see that training with AdaReg leads to an estimator of W that has lower stable rank and smaller spectral norm, which explains why it achieves a better generalization performance.

Furthermore, this observation holds on the SARCOS datasets as well. For the SARCOS dataset, the weight matrix being regularized is of dimension 100×7. Again, we compare the results using three methods: MTL, MTL-WeightDecay and MTL-AdaReg. As can be observed from Table 2, compared with the weight decay regularization, AdaReg substantially reduces both the stable rank and the spectral norm of learned weight matrix, which also helps to explain why MTL-AdaReg generalizes better compared with MTL and MTL-WeightDecay.

Table 2: Stable rank and spectral norm on SARCOS.

	MTL	**MTL-WeightDecay**	**MTL-AdaReg**
Stable Rank	4.48	4.83	**2.88**
Spectral Norm	0.96	0.92	**0.70**

Correlation Matrix: To verify that AdaReg imposes the effect of "sharing statistical strength" during training, we visualize the weight matrix of the softmax layer by computing the corresponding correlation matrix, as shown in Fig. 5. In Fig. 5, darker color means stronger correlation. We conduct two experiments with training size 600 and 60,000 respectively. As we can observe, training with AdaReg leads to weight matrix with stronger correlations, and this effect is more evident when the training set is large. This is consistent with our analysis of sharing statistical strengths. As a sanity check, from Fig. 5 we can also see that similar digits, e.g., 1 and 7, share a positive correlation while dissimilar ones, e.g., 1 and 8, share a negative correlation.

5 Related Work

The Empirical Bayes Method vs Bayesian Neural Networks Despite the name, empirical Bayes method is in fact a frequentist approach to obtain estimator with favorable properties. On the other hand, truly Bayesian inference would instead put a posterior distribution over model weights to characterize the uncertainty during training [2, 20, 30]. However, due to the complexity of nonlinear neural networks, analytic posterior is not available, hence strong independent assumptions over model weight have to be made in order to achieve computationally tractable variational solution. Typically, both the prior and the variational posterior are assumed to fully factorize over model weights. As an exception, Louizos and Welling [29], Sun et al. [40] seek to learn Bayesian neural nets where they approximate the intractable posterior distribution using matrix-variate Gaussian distribution. The prior for weights are still assumed to be known and fixed. As a comparison, we use matrix-variate Gaussian as the prior distribution and we learn the hyperparameter in the prior from data. Hence our method does not belong to Bayesian neural nets: we instead use the empirical Bayes principle to derive adaptive regularization method in order to have better generalization, as done in [4, 35].

Regularization Techniques in Deep Learning Different kinds of regularization approaches have been studied and designed for neural networks, e.g., weight decay [26], early stopping [5], Dropout [39] and the more recent DeCov [6] method. BN was proposed to reduce the internal covariate shift during training, but recently it has been empirically shown to actually smooth the landscape of the loss function [37]. As a comparison, we propose AdaReg as an adaptive regularization method, with the aim to reduce overfitting by allowing neurons to share statistical strengths. From the optimization perspective, learning the row and column covariance matrices help to converge to better local optimum that also generalizes better.

Kronecker Factorization in Optimization The Kronecker factorization assumption has also been applied in the literature of neural networks to approximate the Fisher information matrix in second-order optimization methods [31, 42]. The main idea here is to approximate the curvature of the loss function's landscape, in order to achieve better convergence speed compared with first-order method while maintaining the tractability of such computation. Different from these work, here in our method we assume a Kronecker factorization structure on the covariance matrix of the prior distribution, not the Fisher information matrix of the log-likelihood function. Furthermore, we also derive closed-form solutions to optimize these factors without any kind of approximations.

6 Conclusion

Inspired by empirical Bayes method, in this paper we propose an adaptive regularization (AdaReg) with matrix-variate normal prior for model parameters in deep neural networks. The prior encourages neurons to borrow statistical strength from other neurons during the learning process, and it provides an effective regularization when training networks on small datasets. To optimize the model, we design an efficient block coordinate descent algorithm to learn both model weights and the covariance structures. Empirically, on three datasets we demonstrate that AdaReg improves generalization by finding better local optima with smaller spectral norms and stable ranks. We believe our work takes an important step towards exploring the combination of ideas from the empirical Bayes literature and rich prediction models like deep neural networks. One interesting direction for future work is to extend the current approach to online setting where we only have access to one training instance at a time, and to analyze the property of such method in terms of regret analysis with adaptive optimization methods.

Acknowledgments

HZ and GG would like to acknowledge support from the DARPA XAI project, contract #FA87501720152 and an Nvidia GPU grant. YT and RS were supported in part by DARPA grant FA875018C0150, DARPA SAGAMORE HR00111990016, Office of Naval Research grant N000141812861, AFRL CogDeCON, and Apple. YT and RS would also like to acknowledge NVIDIA's GPU support. Last, we thank Denny Wu for suggestions on exploring and analyzing our algorithm in terms of stable rank.

References

[1] José M Bernardo and Adrian FM Smith. Bayesian theory, 2001.

[2] Charles Blundell, Julien Cornebise, Koray Kavukcuoglu, and Daan Wierstra. Weight uncertainty in neural networks. *arXiv preprint arXiv:1505.05424*, 2015.

[3] Stephen Boyd and Lieven Vandenberghe. *Convex optimization*. Cambridge university press, 2004.

[4] Philip J Brown, James V Zidek, et al. Adaptive multivariate ridge regression. *The Annals of Statistics*, 8(1):64–74, 1980.

[5] Rich Caruana, Steve Lawrence, and C Lee Giles. Overfitting in neural nets: Backpropagation, conjugate gradient, and early stopping. In *Advances in neural information processing systems*, pages 402–408, 2001.

[6] Michael Cogswell, Faruk Ahmed, Ross Girshick, Larry Zitnick, and Dhruv Batra. Reducing overfitting in deep networks by decorrelating representations. *arXiv preprint arXiv:1511.06068*, 2015.

[7] John Duchi, Elad Hazan, and Yoram Singer. Adaptive subgradient methods for online learning and stochastic optimization. *Journal of Machine Learning Research*, 12(Jul):2121–2159, 2011.

[8] Bradley Efron. *Large-scale inference: empirical Bayes methods for estimation, testing, and prediction*, volume 1. Cambridge University Press, 2012.

[9] Bradley Efron and Trevor Hastie. *Computer age statistical inference*, volume 5. Cambridge University Press, 2016.

[10] Bradley Efron and Carl Morris. Stein's estimation rule and its competitors—an empirical Bayes approach. *Journal of the American Statistical Association*, 68(341):117–130, 1973.

[11] Bradley Efron and Carl Morris. Stein's paradox in statistics. *Scientific American*, 236(5): 119–127, 1977.

[12] Andrew Gelman, John B Carlin, Hal S Stern, David B Dunson, Aki Vehtari, and Donald B Rubin. *Bayesian data analysis*. CRC press, 2013.

[13] Gene H Golub, Michael Heath, and Grace Wahba. Generalized cross-validation as a method for choosing a good ridge parameter. *Technometrics*, 21(2):215–223, 1979.

[14] Priya Goyal, Piotr Dollár, Ross Girshick, Pieter Noordhuis, Lukasz Wesolowski, Aapo Kyrola, Andrew Tulloch, Yangqing Jia, and Kaiming He. Accurate, large minibatch sgd: training imagenet in 1 hour. *arXiv preprint arXiv:1706.02677*, 2017.

[15] Erin Grant, Chelsea Finn, Sergey Levine, Trevor Darrell, and Thomas Griffiths. Recasting gradient-based meta-learning as hierarchical bayes. *arXiv preprint arXiv:1801.08930*, 2018.

[16] Arjun K Gupta and Daya K Nagar. *Matrix variate distributions*. Chapman and Hall/CRC, 2018.

[17] Vineet Gupta, Tomer Koren, and Yoram Singer. A unified approach to adaptive regularization in online and stochastic optimization. *arXiv preprint arXiv:1706.06569*, 2017.

[18] Elad Hazan, Amit Agarwal, and Satyen Kale. Logarithmic regret algorithms for online convex optimization. *Machine Learning*, 69(2-3):169–192, 2007.

[19] Kaiming He, Xiangyu Zhang, Shaoqing Ren, and Jian Sun. Deep residual learning for image recognition. In *Proceedings of the IEEE conference on computer vision and pattern recognition*, pages 770–778, 2016.

[20] José Miguel Hernández-Lobato and Ryan Adams. Probabilistic backpropagation for scalable learning of bayesian neural networks. In *International Conference on Machine Learning*, pages 1861–1869, 2015.

[21] Elad Hoffer, Itay Hubara, and Daniel Soudry. Train longer, generalize better: closing the generalization gap in large batch training of neural networks. In *Advances in Neural Information Processing Systems*, pages 1731–1741, 2017.

[22] Sergey Ioffe and Christian Szegedy. Batch normalization: Accelerating deep network training by reducing internal covariate shift. *arXiv preprint arXiv:1502.03167*, 2015.

[23] William James and Charles Stein. Estimation with quadratic loss. In *Proceedings of the fourth Berkeley symposium on mathematical statistics and probability*, volume 1, pages 361–379, 1961.

[24] Nitish Shirish Keskar, Dheevatsa Mudigere, Jorge Nocedal, Mikhail Smelyanskiy, and Ping Tak Peter Tang. On large-batch training for deep learning: Generalization gap and sharp minima. *arXiv preprint arXiv:1609.04836*, 2016.

[25] Alex Krizhevsky and Geoffrey Hinton. Learning multiple layers of features from tiny images. 2009.

[26] Anders Krogh and John A Hertz. A simple weight decay can improve generalization. In *Advances in neural information processing systems*, pages 950–957, 1992.

[27] Yann LeCun, Yoshua Bengio, and Geoffrey Hinton. Deep learning. *nature*, 521(7553):436, 2015.

[28] Mingsheng Long, Zhangjie Cao, Jianmin Wang, and S Yu Philip. Learning multiple tasks with multilinear relationship networks. In *Advances in Neural Information Processing Systems*, pages 1594–1603, 2017.

[29] Christos Louizos and Max Welling. Structured and efficient variational deep learning with matrix gaussian posteriors. In *International Conference on Machine Learning*, pages 1708–1716, 2016.

[30] David JC MacKay. A practical bayesian framework for backpropagation networks. *Neural computation*, 4(3):448–472, 1992.

[31] James Martens and Roger Grosse. Optimizing neural networks with kronecker-factored approximate curvature. In *International conference on machine learning*, pages 2408–2417, 2015.

[32] Sanjay Mehrotra. On the implementation of a primal-dual interior point method. *SIAM Journal on optimization*, 2(4):575–601, 1992.

[33] Vinod Nair and Geoffrey E Hinton. Rectified linear units improve restricted boltzmann machines. In *Proceedings of the 27th international conference on machine learning (ICML-10)*, pages 807–814, 2010.

[34] Behnam Neyshabur, Srinadh Bhojanapalli, David McAllester, and Nathan Srebro. A pac-bayesian approach to spectrally-normalized margin bounds for neural networks. *arXiv preprint arXiv:1707.09564*, 2017.

[35] Samuel D Oman. A different empirical bayes interpretation of ridge and stein estimators. *Journal of the Royal Statistical Society: Series B (Methodological)*, 46(3):544–557, 1984.

[36] Herbert Robbins. An empirical bayes approach to statistics. Technical report, Columbia University, New York City, United States, 1956.

[37] Shibani Santurkar, Dimitris Tsipras, Andrew Ilyas, and Aleksander Madry. How does batch normalization help optimization?(no, it is not about internal covariate shift). *arXiv preprint arXiv:1805.11604*, 2018.

[38] Karen Simonyan and Andrew Zisserman. Very deep convolutional networks for large-scale image recognition. *arXiv preprint arXiv:1409.1556*, 2014.

[39] Nitish Srivastava, Geoffrey Hinton, Alex Krizhevsky, Ilya Sutskever, and Ruslan Salakhutdinov. Dropout: A simple way to prevent neural networks from overfitting. *The Journal of Machine Learning Research*, 15(1):1929–1958, 2014.

[40] Shengyang Sun, Changyou Chen, and Lawrence Carin. Learning structured weight uncertainty in bayesian neural networks. In *Artificial Intelligence and Statistics*, pages 1283–1292, 2017.

[41] Sethu Vijayakumar and Stefan Schaal. Locally weighted projection regression: Incremental real time learning in high dimensional space. In *Proceedings of the Seventeenth International Conference on Machine Learning*, pages 1079–1086. Morgan Kaufmann Publishers Inc., 2000.

[42] Guodong Zhang, Shengyang Sun, David Duvenaud, and Roger Grosse. Noisy natural gradient as variational inference. *arXiv preprint arXiv:1712.02390*, 2017.

[43] Han Zhao, Otilia Stretcu, Alex Smola, and Geoff Gordon. Efficient multitask feature and relationship learning. In *Proceedings of the Thirty-Fifth Conference on Uncertainty in Artificial Intelligence*. AUAI Press, 2019.

Appendix

In this appendix we present missing proofs in the main paper. We also provide detailed description of our experiments.

A Detailed Derivation and Proofs of Our Algorithm

We first show that the optimization problem (9) is convex:

Proposition 1. The optimization problem (9) is convex.

Proof. It is clear that the objective function is convex: the trace term is linear in Ω_r and it is well-known that the $\log\det(\cdot)$ is concave in the positive definite cone [3], hence it trivially follows that $\text{Tr}(\Omega_r W \Omega_c W^T) - d\log\det(\Omega_r)$ is convex in Ω_r.

It remains to show that the constraint set is also convex. Let Ω_1, Ω_2 be any feasible points, i.e., $uI_p \preceq \Omega_1 \preceq vI_p$ and $uI_p \preceq \Omega_2 \preceq vI_p$. Let $\forall t \in (0,1)$, we have:

$$||t\Omega_1 + (1-t)\Omega_2||_2 \leq t||\Omega_1||_2 + (1-t)||\Omega_2||_2 \leq tv + (1-t)v = v,$$

where we use $||\cdot||_2$ to denote the spectral norm of a matrix. Now since both Ω_1 and Ω_2 are positive definite, the spectral norm is also the largest eigenvalue, hence this shows that $t\Omega_1 + (1-t)\Omega_2 \preceq vI_p$.

To show the other direction, we use the Courant-Fischer characterization of eigenvalues. Let $\lambda_{\text{min}}(A)$ denote the minimum eigenvalue of a real symmetric matrix A, then by the Courant-Fischer min-max theorem, we have:

$$\lambda_{\text{min}}(A) := \min_{\mathbf{x}\neq 0, ||\mathbf{x}||_2=1} ||A\mathbf{x}||_2.$$

For the matrix $t\Omega_1 + (1-t)\Omega_2$, let $\mathbf{x}^*$ be the vector corresponding to the minimum eigenvalue, hence we have:

$$\begin{aligned}
\lambda_{\text{min}}(t\Omega_1 + (1-t)\Omega_2) &= \min_{\mathbf{x}\neq 0, ||\mathbf{x}||_2=1} ||(t\Omega_1 + (1-t)\Omega_2)\mathbf{x}||_2 \\
&= (t\Omega_1 + (1-t)\Omega_2)\mathbf{x}^* \\
&\geq t\lambda_{\text{min}}(\Omega_1) + (1-t)\lambda_{\text{min}}(\Omega_2) \\
&\geq tu + (1-t)u \\
&= u,
\end{aligned}$$

which also means that $t\Omega_1 + (1-t)\Omega_2 \succeq uI_p$, and this completes the proof. ■

We now give the proof of Lemma 1 in our main paper:

Lemma 1. Let $\Omega_r \in \mathcal{C}$, then $\mathcal{N}_{\mathcal{C}}(\Omega_r) = -\mathcal{N}_{\mathcal{C}}(\Omega_r^{-1})$.

Proof. Let $S \in \mathcal{N}_{\mathcal{C}}(\Omega_r)$. We want to show $-S \in \mathcal{N}_{\mathcal{C}}(\Omega_r^{-1})$. By definition of the normal cone, since $S \in \mathcal{N}_{\mathcal{C}}(\Omega_r)$, we have:

$$\text{Tr}(SZ) \leq \text{Tr}(S\Omega_r), \quad \forall Z \in \mathcal{C}$$

Now realize that $\Omega_r \in \mathcal{C}$ and $\mathcal{C}$ is a compact set, it follows Ω_r is the solution of the following linear program:

$$\max \quad \text{Tr}(SZ), \qquad \text{subject to} \quad Z \in \mathcal{C}$$

Since both S and Z are real symmetric matrix, we can decompose them as $Z := Q_Z \Lambda_Z Q_Z^T$ and $S := Q_S \Lambda_S Q_S^T$, where both Q_Z, Q_S are orthogonal matrices and Λ_Z, Λ_S are diagonal matrices with the corresponding eigenvalues in decreasing order. Plug them into the objective function, we have:

$$\text{Tr}(SZ) = \text{Tr}(Q_S \Lambda_S Q_S^T Q_Z \Lambda_Z Q_Z^T) = \text{Tr}(\Lambda_S Q_S^T Q_Z \Lambda_Z Q_Z^T Q_S).$$

Define $K := Q_S^T Q_Z$ and $D = K \circ K$, where we use $\circ$ to denote the Hadamard product between two matrices. Since both Q_S and Q_Z are orthogonal matrices, we know that K is also orthogonal, which implies:

$$\sum_{j=1}^{p} D_{ij} = 1, \forall i \in [p], \quad \text{and} \quad \sum_{i=1}^{p} D_{ij} = 1, \forall j \in [p].$$

As a result, D is a doubly stochastic matrix and we can further simplify the objective function as:

$$\operatorname{Tr}(\Lambda_S Q_S^T Q_Z \Lambda_Z Q_Z^T Q_S) = \operatorname{Tr}(\Lambda_S K \Lambda_Z K^T) = \lambda_S^T D \lambda_Z = \sum_{i,j=1}^{p} \lambda_{S,i} D_{ij} \lambda_{Z,j},$$

where λ_S and λ_Z are p dimensional vectors that contain the eigenvalues of S and Z in decreasing order, respectively. Now for any λ_S and λ_Z in decreasing order, we have:

$$u\sum_{i=1}^{p} \lambda_{S,i} \leq \sum_{i=1}^{p} \lambda_{S,i}\lambda_{Z,1+p-i} \leq \sum_{i,j=1}^{p} \lambda_{S,i} D_{ij} \lambda_{Z,j} \leq \sum_{i=1}^{p} \lambda_{S,i}\lambda_{Z,i} \leq v\sum_{i=1}^{p} \lambda_{S,i} \tag{11}$$

From (11), in order for Ω_r to maximize the linear program, it must hold that $D = K = I_p$ and all the eigenvalues of Ω_r are v. But due to the assumption that $uv = 1$, in this case we also know that all the eigenvalues of Ω_r^{-1} are $1/v = u$, hence Ω_r^{-1} also minimizes the above linear program, which implies:

$$\operatorname{Tr}(S\Omega_r^{-1}) \leq \operatorname{Tr}(SZ), \quad \forall Z \in \mathcal{C} \Leftrightarrow \operatorname{Tr}(-S(Z - \Omega_r^{-1})) \leq 0 \quad \forall Z \in \mathcal{C}.$$

In other words, we have $-S \in \mathcal{N}_{\mathcal{C}}(\Omega_r^{-1})$. Using exactly the same arguments it is clear to see that the other direction also holds, hence we have $\mathcal{N}_{\mathcal{C}}(\Omega_r) = -\mathcal{N}_{\mathcal{C}}(\Omega_r^{-1})$. ■

Here we proceed to derive the projection operator:

Theorem 1. Let $\widetilde{\Omega_r} \in \mathbb{S}^p$ with eigendecomposition as $\widetilde{\Omega_r} = Q\Lambda Q^T$ and $\operatorname{Proj}_{\mathcal{C}}(\cdot)$ be the Euclidean projection operator onto $\mathcal{C}$, then $\operatorname{Proj}_{\mathcal{C}}(\widetilde{\Omega_r}) = Q\mathbb{T}_{[u,v]}(\Lambda)Q^T$.

Proof. Since $\Omega_r \in \mathcal{C}$ is real and symmetric, we can reparametrize Ω_r as $\Omega_r := U\Lambda_{\Omega_r}U^T$ where U is an orthogonal matrix and Λ_{Ω_r} is a diagonal matrix whose entries corresponds to the eigenvalues of Ω_r. Recall that U corresponds to a rigid transformation that preserves length, so we have:

$$||\Omega_r - \widetilde{\Omega_r}||_F^2 = ||U\Lambda_{\Omega_r}U^T - UU^T\widetilde{\Omega_r}UU^T||_F^2 = ||\Lambda_{\Omega_r} - U^T\widetilde{\Omega_r}U||_F^2 \tag{12}$$

Define $B := U^T\widetilde{\Omega_r}U$. Now by using the fact that $\widetilde{\Omega_r}$ can be eigendecomposed as $\widetilde{\Omega_r} = Q\Lambda Q^T$, we can further simplify (12) as:

$$||\Lambda_{\Omega_r} - U^T\widetilde{\Omega_r}U||_F^2 = \sum_{i\in[p]}(\Lambda_{\Omega_r,ii} - B_{ii})^2 + \sum_{i\neq j} B_{ij}^2 \geq \sum_{i\in[p]}(\Lambda_{\Omega_r,ii} - B_{ii})^2 \geq \sum_{i\in[p]}(\mathbb{T}_{[u,v]}(B_{ii}) - B_{ii})^2,$$

where the last inequality holds because $u \leq \Lambda_{\Omega_r,ii} \leq v, \forall i \in [p]$. In order to achieve the first equality, $B = U^T\widetilde{\Omega_r}U$ should be a diagonal matrix, which means $U^TQ = I_p \Leftrightarrow U = Q$. In this case, $\operatorname{diag}(B) = \Lambda$. To achieve the second equality, simply let $\Lambda_{\Omega_r} = \mathbb{T}_{[u,v]}(\operatorname{diag}(B)) = \mathbb{T}_{[u,v]}(\Lambda)$, which completes the proof. ■

B More Experiments

In this section we first describe the network structures used in our main experiments and present more experimental results.

B.1 Network Structures

Multiclass Classification (MNIST & CIFAR10): We use a convolutional neural network as our baseline model. The network used in the experiment has the following structure: $\mathsf{CONV}_{5\times5\times1\times10}$-$\mathsf{CONV}_{5\times5\times10\times20}$-$\mathsf{FC}_{320\times50}$-$\mathsf{FC}_{50\times10}$. The notation $\mathsf{CONV}_{5\times5\times1\times10}$ denotes a convolutional layer with kernel size 5×5 from depth 1 to 10; the notation $\mathsf{FC}_{320\times50}$ denotes a fully connected layer with size 320×50. Similarly, CIFAR10 considers the structure: $\mathsf{CONV}_{5\times5\times3\times10}$-$\mathsf{CONV}_{5\times5\times10\times20}$-$\mathsf{FC}_{500\times500}$-$\mathsf{FC}_{500\times500}$-$\mathsf{FC}_{500\times10}$.

Multitask Regression (SARCOS): The network structure is given by $\mathsf{FC}_{21\times256}$-$\mathsf{FC}_{256\times100}$-$\mathsf{FC}_{100\times7}$.

B.2 Combination

As discussed in the main text, combining the proposed AdaReg with BN can further improve the generalization performance, due to the complementary effects between these two approaches: BN helps smoothing the landscape of the loss function while AdaReg also changes the curvature via the row and column covariance matrices (see Fig. 6).

On the other hand, we do not observe significant difference when combining AdaReg with Dropout on this dataset. While we are not clear what is the exact reason for this effect, we conjecture this is due to the fact that Dropout works as a regularizer that prevents coadaptation while AdaReg instead encourages neurons to learn from each other.

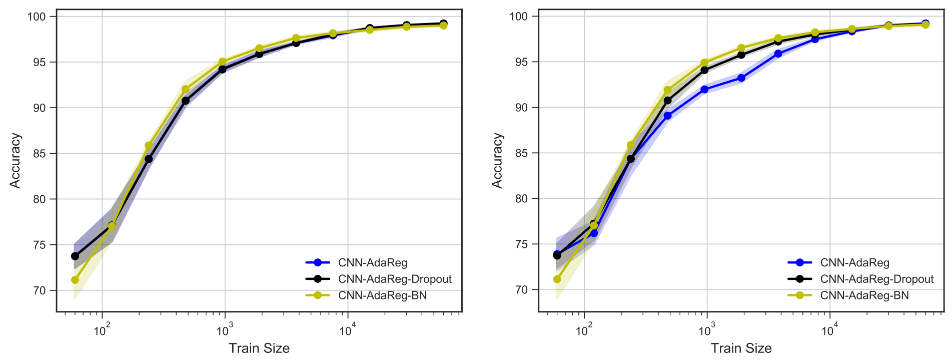

(a) Batch size = 256.

(b) Batch size = 2048.

Figure 6: Combine AdaReg with BN and Dropout on MNIST.

B.3 Ablations

In all the experiments, the AdaReg algorithm is performed on the softmax layer. Here, we study the effects of applying AdaReg algorithm in all CONV/FC layers, all CONV layers, all FC layers, and the last FC layer (i.e., softmax layer). We first discuss how we handle the convolutions in our AdaReg algorithm. Consider a convolutional layer with {input channel, output channel, kernel width, kernel height} being $\{a, b, k_w, k_h\}$, we vectorize the original 4-D tensor to be a 2-D matrix of size $ak_wk_h \times b$. The AdaReg algorithm can therefore be directly applied on this transformed matrix. Next, we perform the experiment on MNIST with batch size 2048 in Fig. 7. The training set size here is chosen as {128, 256, 512, 1024, 2048, 4096, 8192, 16384, 32768, 60000}.

We find that simply applying the AdaReg algorithm in the softmax layer reaches best generalization as comparing to applying AdaReg on more layers. The improvement is more obvious when the training set size is small. We argue that neural networks can be realized as a combination of a complex nonlinear transformation (i.e., feature extraction) and a linear model (i.e., softmax layer). Since AdaReg represents a correlation learning in the weight matrix, it implies that implicit correlations of neurons can also be discovered. In the real world setting, different tasks should be correlated. Therefore, applying AdaReg in the linear model shall improve the model performance by discovering these tasks correlations. On the contrary, the nonlinear features should be decorrelated for the purpose of generalization. Hence, applying AdaReg in previous layers may lead to adversarial effect.

B.4 Covariance matrices in the prior

One byproduct that AdaReg brings to us is the learned row and column covariance matrices, which can be used in exploratory data analysis to understand the correlations between learned features and different output tasks. To this end, we visualize both the row and column covariance matrices in Fig. 8. The two covariance matrices on the first row correspond to the ones learned on a training set with 600 instances while the two on the second row are trained with the full dataset on MNIST.

From Fig. 8 we can make the following observations: the structure of both covariance matrices become more evident when trained with larger dataset, and this is consistent with the Bayesian principle because more data provide more evidence. Second, we observe in our experiments that the

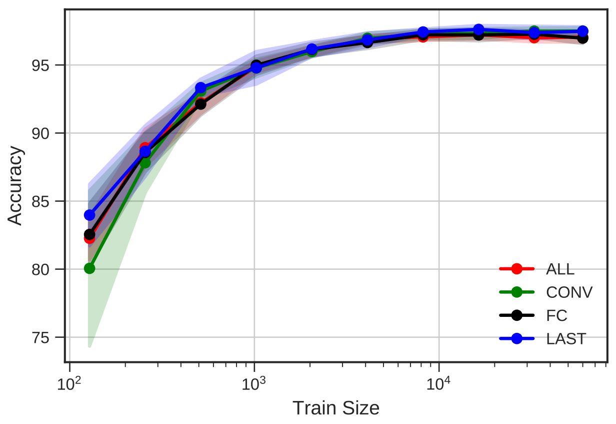

Figure 7: Applying AdaReg on different layers in neural networks for MNIST with batch size 2048.

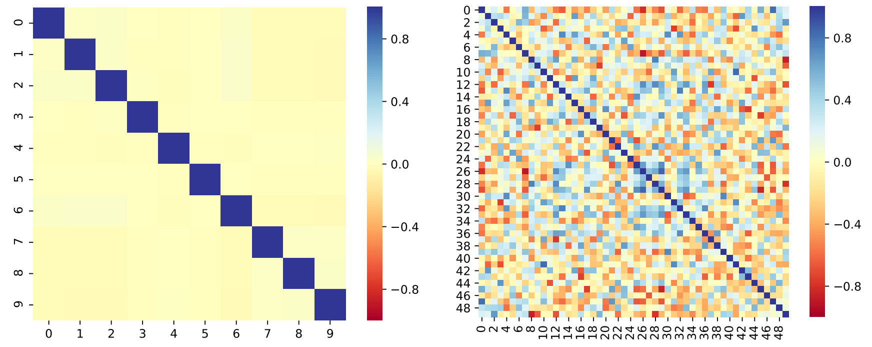

(a) Row Cov. matrix trained on 600 instances.

(b) Column Cov. matrix trained on 600 instances.

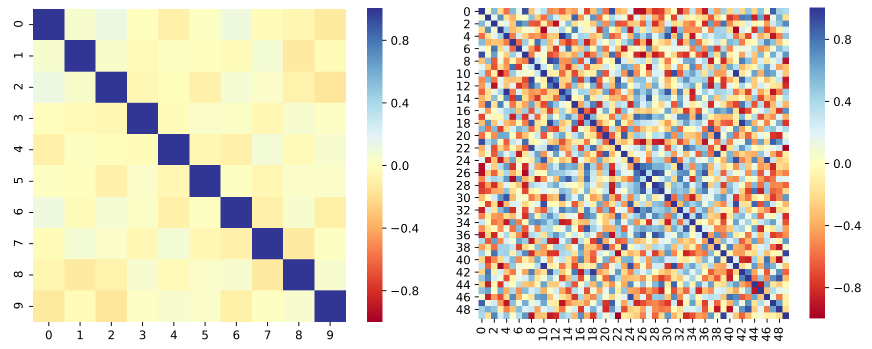

(c) Row Cov. matrix trained on 60,000 instances.

(d) Column Cov. matrix trained on 60,000 instances.

Figure 8: Recovered row covariance matrix Σ_r and column covariance matrix Σ_c in the prior distribution on MNIST.

variances of both matrices are small. In fact, the variance of the row covariance matrix Σ_r achieves the lower bound limit u at convergence. Lastly, comparing the row covariance matrix Σ_r in Fig. 8 with the one computed from model weights in Fig. 5, we can see that both matrices exhibit the same correlation patterns, except that the one obtained from model weights are more evident, which is due to the fact that model weights are closer to data evidence than the row covariance matrix in the Bayesian hierarchy.

On the other hand, the column covariance matrix in Fig. 8 also exhibit rich correlations between the learned features, e.g., the neurons in the penultimate layer. Again, with more data, these patterns become more evident.

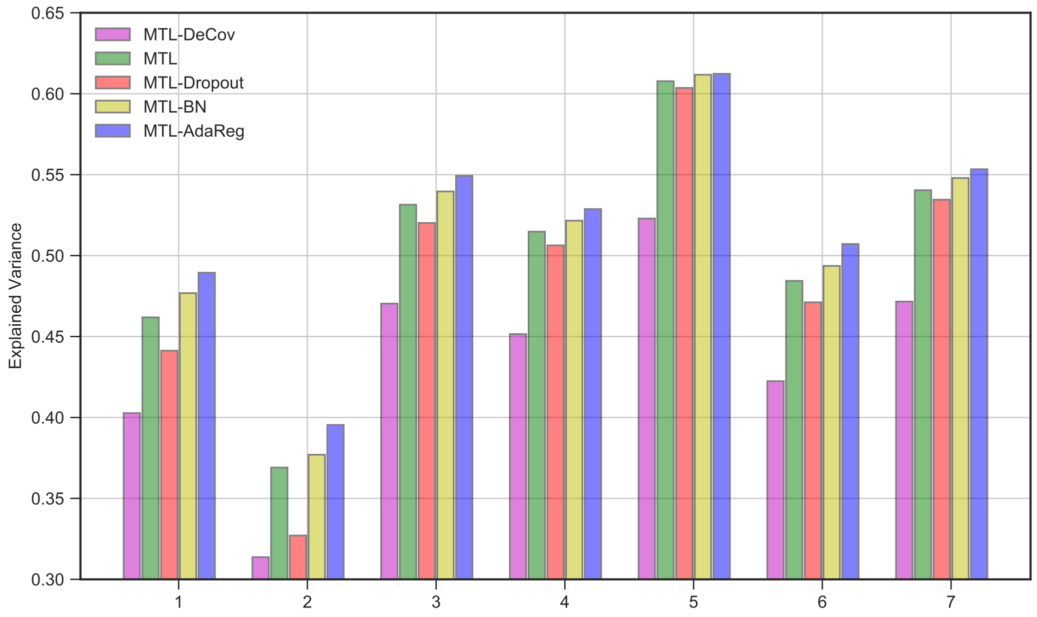

Figure 9: Explained variance of different methods on 7 regression tasks from the SARCOS dataset.